INTERNATIONAL JOURNAL FOR NUMERICAL AND ANALYTICAL METHODS IN GEOMECHANICS, VOL. 10, 633–652 (1986)

GENERALIZED DISPLACEMENTS OF A RIGID ELLIPTICAL ANCHOR EMBEDDED AT A BI-MATERIAL GEOLOGICAL INTERFACE

A. P. S. SELVADURAI† AND M. C. AU‡

Department of Civil Engineering, Carleton University, Ottawa, Ontario, Canada

SUMMARY

The present paper examines the class of problems related to a flat rigid anchoring region which is embedded at a geological interface. The analysis focuses on the evaluation of the elastic stiffness of the embedded anchor. A boundary element technique is used to estimate the axial, rotational and translational stiffnesses of the anchor. These estimates are compared with a set of bounds which are evaluated in exact closed form. These bounds are obtained by invoking kinematic and/or traction constraints at the geological interface. The numerical results presented in the paper illustrate the manner in which the various stiffnesses of the anchoring region are influenced by the elastic properties of the surrounding geological media.

INTRODUCTION

Problems which deal with rigid or flexible objects embedded in elastic media are of importance to geomechanical applications. The embedded inhomogeneity serves as a useful mechanical model of a foundation or an anchor region deeply embedded in the geological material. Several investigators[1–6] have therefore examined problems related to the loading of objects embedded in elastic and transversely isotropic elastic media. In this paper, we examine the group of problems related to the generalized loading of a rigid flat anchor with an elliptical planform which is embedded at a bi-material elastic interface. Such a flat rigid anchoring region can be formed at a bi-material geological interface by hydraulic fracturing effects of pressure injected grouting (Figure 1). The rigid anchor region represents the hardened cement grout or a resinous material. The elastic stiffness of these anchoring regions is important to the estimation of the efficiency of the anchoring system.

The present paper focuses on the determination of the axial, rotational and translational stiffnesses of a rigid elliptical disc anchor which is embedded in bonded contact at a bi-material geological interface. The elliptical planform is a convenient geometrical shape which can be used to model an anchor region obtained by fluid-induced fracture or separation of the interface. The choice of an elliptical anchor geometry, however, makes the analytical solution of the elastostatic boundary value problem inordinately complicated. The exact formulation of the linear elastostatic problem related to rigid disc anchor embedded at a bi-material region yields a complicated set of simultaneous singular integral equations which cannot be solved in an exact fashion. For this

† Professor and Chairman.
‡ Post Doctoral Research Fellow.

0363–9061/86/060633–20$10.00

Received 22 February 1984
Revised 11 September 1985

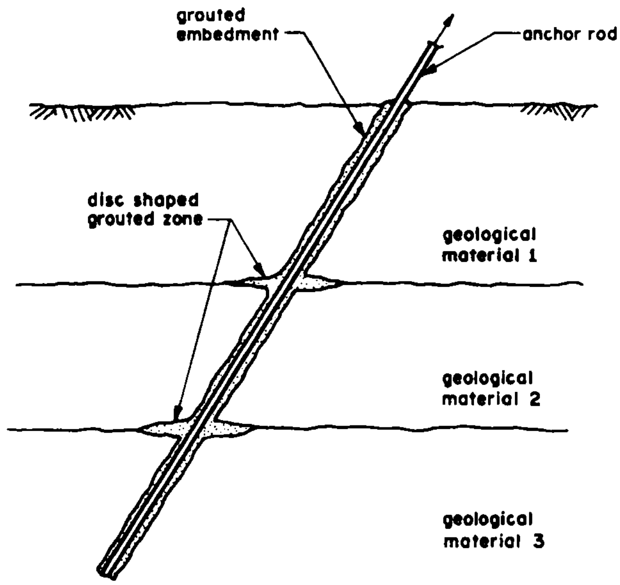

Figure 1. Disc-shaped anchor zones embedded at bi-material geological interfaces

reason it is desirable to explore alternative methods which can be employed to estimate the elastic stiffness of the anchor embedded at the bi-material interface. To this end the boundary element technique is used to evaluate the stiffnesses of the rigid anchor embedded at the bi-material interface. These numerical results are compared with a set of analytically derived bounds obtained by invoking kinematic and/or traction constraints at the interface. The upper bound assumes inextensibility of the geological interface and the lower bound imposes a bi-lateral smooth condition at the interface. The influence of the elasticity mismatch between the geological media on the elastic stiffnesses is illustrated by appeal to numerical results.

FUNDAMENTAL EQUATIONS

A rigid elliptical disc shaped anchor is at a bi-material elastic interface as shown in Figure 2. The anchor is located in the plane $z = 0$ and the origin of co-ordinates coincides with the centre of the elliptical region. The inclusion region is denoted by S^* and the interface region exterior to the inclusion is denoted by $\tilde{S}$. Referring to Figure 3, the total surface area Γ of the solid is given by

$$\Gamma = \Gamma^1 \cup \Gamma^2 = S^* \cup \tilde{S} \cup S^{(1)} \cup S^{(2)} \tag{1}$$

where $S^{(\alpha)}$ $(\alpha = 1, 2)$ are the exterior surfaces of the regions α and Γ^α $(\alpha = 1, 2)$ are the total surface areas of the regions α. Here and in the sequel, the Greek subscripts or superscripts will refer the material regions 1 and 2, respectively.

For three-dimensional problems in elasticity, the displacement components u_i^α $(i = x, y, z)$ in a medium free of body forces are governed by the Navier equations

$$G_\alpha \nabla^2 u_i^{(\alpha)} + (\lambda_\alpha + G_\alpha) u_{k,ki}^{(\alpha)} = 0 \tag{2}$$

where G_α and λ_α are Lamé's constants; $\lambda_\alpha = 2G_\alpha \nu_\alpha/(1 - 2\nu_\alpha)$; G_α are the shear moduli; ν_α are Poisson's ratios and ∇^2 is Laplace's operator referred to the rectangular Cartesian co-ordinate

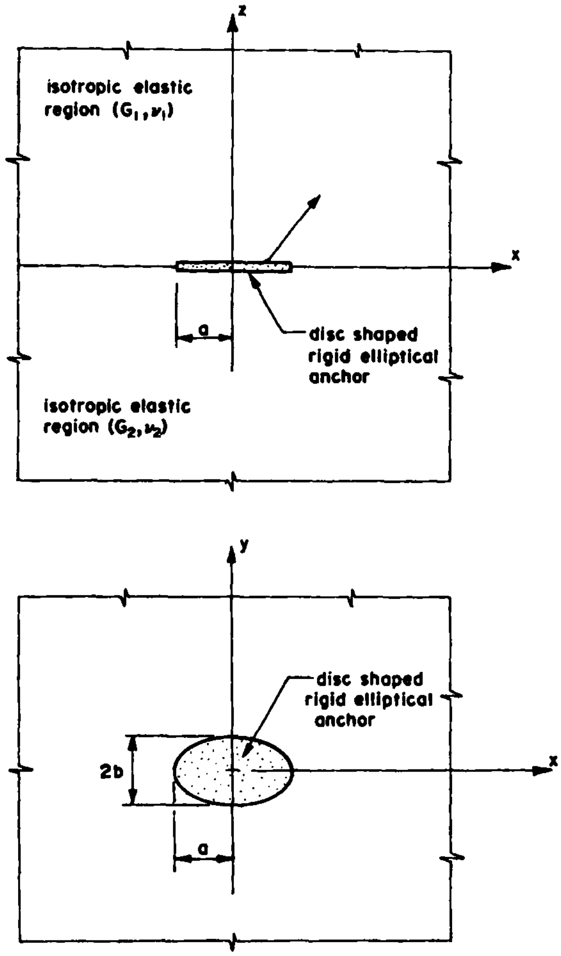

Figure 2. Rigid disc-shaped elliptical anchor region embedded at a bi-material elastic interface

system. The displacement equations (2) can be solved by using a variety of stress and displacement function techniques. Detailed accounts of these representations are given by Truesdell,[7] Gurtin[8] and Gladwell.[9] For example in the generalized Papkovich–Neuber representation the solution for $u_i^{(\alpha)}$ can be expressed in terms of four stress functions $\phi_i^{(\alpha)}$ and $\phi_0^{(\alpha)}$ in the form

$$2G_\alpha u_i^{(\alpha)} = (3 - 4\nu_\alpha)\phi_i^{(\alpha)} - x_j\phi_{j,i}^{(\alpha)} - \phi_{0,i}^{(\alpha)} \tag{3}$$

where $x_1 = x$, $x_2 = y$ and $x_3 = z$. Once the displacement components are known, the stress components in the isotropic elastic media ($\alpha = 1, 2$) can be obtained from the stress–displacement relationships

$$\sigma_{ij}^{(\alpha)} = \lambda_\alpha \delta_{ij} u_{k,k}^{(\alpha)} + G_\alpha\{u_{i,j}^{(\alpha)} + u_{j,i}^{(\alpha)}\} \tag{4}$$

where δ_{ij} is Kronecker's delta function. The traction boundary conditions on a surface are given by

$$t_i^{(\alpha)} = \sigma_{ij}^{(\alpha)} n_j^{(\alpha)} \tag{5}$$

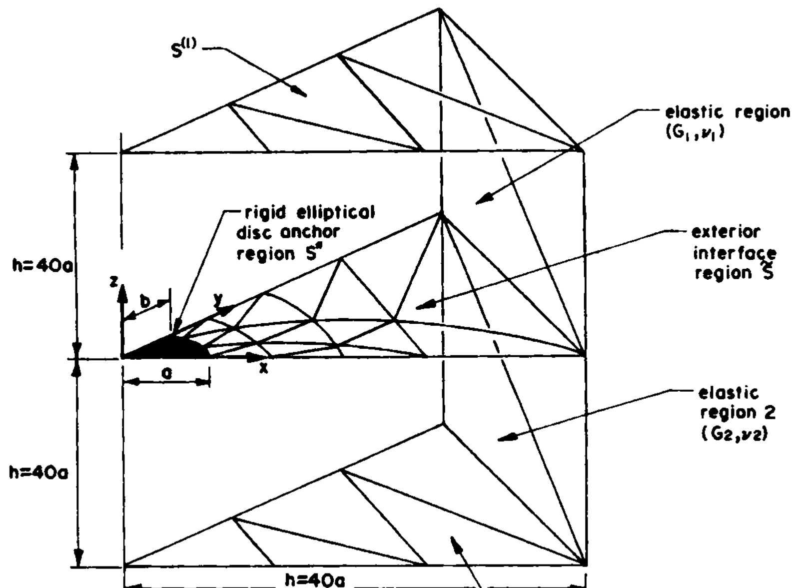

(a) boundary element discretization of the bi-material elastic region

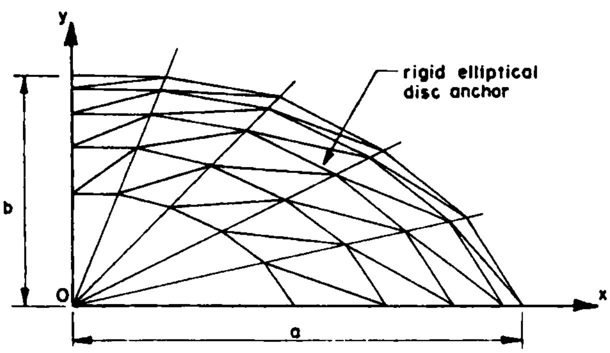

(b) boundary element discretization of the elliptical disc anchor region

Figure 3. Boundary element discretizations

where $n_j^{(\alpha)}$ is the outward unit normal to the surface in the region α. In the class of problems considered in this paper, the rigid elliptical anchor is embedded in full bonded contact at the bi-material elastic region. In the anchor region the displacements are prescribed; i.e.

$$u_i^{(1)}(x, y, 0^+) = u_i^{(2)}(x, y, 0^-) = \delta_i(x, y); \qquad (x, y) \in S^* \tag{6}$$

where $\delta_i(x, y)$ are the prescribed displacements. The superscripts $(\ )^+$ and $(\ )^-$ refer to the variables associated with the halfspace regions $z > 0$ and $z < 0$, respectively. For complete continuity in the exterior bi-material interface ($\tilde{S}$)

$$\begin{aligned} u_i^{(1)}(x, y) &= u_i^{(2)}(x, y) = u_i(x, y); \qquad (x, y) \in \tilde{S} \\ t_i^{(1)}(x, y) &= -t_i^{(2)}(x, y) = t_i(x, y); \qquad (x, y) \in \tilde{S} \end{aligned} \tag{7}$$

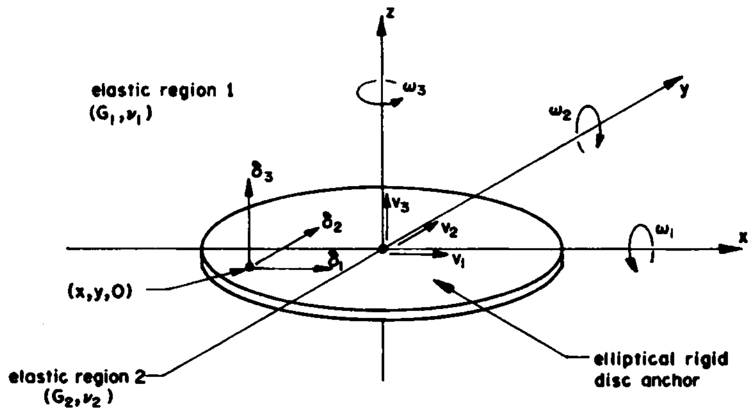

Figure 4. Generalized displacements of the rigid elliptical disc anchor

In general, the displacement vector at any point within the anchor region can be represented in the form

$$u_i = v_i + \varepsilon_{ijk}\omega_j r_k \tag{8}$$

where ε_{ijk} is the alternating tensor; $r_k = (x_k - x_k^*)$; v_i is the translation vector of the rigid anchor at the location x_k^* and ω_i is the rotation vector of the rigid anchor about the cartesian axes located at x_k^*. For a disc anchor which occupies the region S^* located at the bi-material interface ($x_3 = z = 0$), the displacement at any point $(x, y) \in S^*$ can be written in the matrix form

$$\{\boldsymbol{\delta}(x,y)\} = [R(x,y)]\{\Delta\} \tag{9}$$

where

$$\{\Delta\} = \{v_1 \ v_2 \ v_3 \ \omega_1 \ \omega_2 \ \omega_3\}^{\mathrm{T}} \tag{10}$$

$$\{\boldsymbol{\delta}(x,y)\} = \{\delta_1(x,y) \ \delta_2(x,y) \ \delta_3(x,y)\}^{\mathrm{T}} \tag{11}$$

and

$$[R(x,y)] = \begin{bmatrix} 1 & 0 & 0 & 0 & 0 & -y \\ 0 & 1 & 0 & 0 & 0 & x \\ 0 & 0 & 1 & y & -x & 0 \end{bmatrix} \tag{12}$$

The physical interpretations of v_i, δ_i and ω_i ($i = 1, 2, 3$) are given in Figure 4.

THE ELASTIC STIFFNESS MATRIX FROM BEM

The elastostatic boundary element formulation for a bi-material region is given by Brebbia[10] and Banerjee and Butterfield.[11] A complete matrix equation can be expressed in relation to variables associated with respective boundary regions $S^{(1)}$, $S^{(2)}$, $\bar{S}$ and S^*, i.e.

$$[\mathbf{H}_{S^{(1)}}, \mathbf{H}_{S^{(2)}}, \mathbf{H}_{\bar{S}}, \mathbf{H}_{S^*}] \begin{bmatrix} \mathbf{u}_{S^{(1)}} \\ \mathbf{u}_{S^{(2)}} \\ \mathbf{u}_{\bar{S}} \\ \mathbf{u}_{S^*} \end{bmatrix} = [\mathbf{M}_{S^{(1)}}, \mathbf{M}_{S^{(2)}}, \mathbf{M}_{\bar{S}}, \mathbf{M}_{S^*}] \begin{bmatrix} \mathbf{t}_{S^{(1)}} \\ \mathbf{t}_{S^{(2)}} \\ \mathbf{t}_{\bar{S}} \\ \mathbf{t}_{S^*} \end{bmatrix} \tag{13}$$

where the [H] and [M] matrices are, respectively, the integrations of the tractions and the displacement fundamental solutions over the element. The displacements at the anchor surface can be obtained in the form

$$\{\mathbf{u}_{S^*}\} = [\mathbf{B}]\{\Delta\} \tag{14}$$

where [B] is obtained from the submatrices $[R(x,y)]$, defined by (9), by considering all elements in S^*. Applying the boundary condition over all elements (14) can be written as

$$[\mathbf{A} \quad -\mathbf{M}_{S^*}]\begin{bmatrix} \chi \\ \mathbf{t}_{S^*} \end{bmatrix} = \{\mathbf{q}_0\} + [\mathbf{Q} \quad \Delta] \tag{15}$$

where $\{\chi\}$ are unknowns on the boundary $S^{(1)} \cup S^{(2)} \cup \bar{S}$ and $[\mathbf{Q}] = -[\mathbf{H}_{S^*}][\mathbf{B}]$.

Upon solution of equation (15), the traction on the anchor surface can be represented in the form

$$\{\mathbf{t}_{S^*}\} = [\mathbf{C}][\mathbf{A} \quad -\mathbf{M}_{S^*}]^{-1}[\{\mathbf{q}_0\} + [\mathbf{Q}]\{\Delta\}] \tag{16}$$

where [C] can be expressed as [Q, I]. For a rigid anchor region, the total force $\{T_0\}$ is given by

$$\{\mathbf{T}_0\} = \int_{S^*} [\mathbf{B}]^{\mathrm{T}}\{\mathbf{t}_{S^*}\}\,\mathrm{d}\Gamma = \{\mathbf{F}_0\} + \{\mathbf{F}\} \tag{17}$$

where $\{\mathbf{F}_0\}$ are the forces transmitted to the inclusion from the boundary $S^{(1)} \cup S^{(2)}$ which are given by

$$\{\mathbf{F}_0\} = \int_{S^*} [\mathbf{B}]^{\mathrm{T}}[\mathbf{C}][\mathbf{A} \quad -\mathbf{M}_{S^*}]^{-1}\{q_0\}\,\mathrm{d}\Gamma \tag{18}$$

Also $\{\mathbf{F}\}$ are the corresponding forces due to the displacement of the inclusion, which are given by

$$\{\mathbf{F}\} = -\int_{S^*} [\mathbf{B}]^{\mathrm{T}}[\mathbf{C}][\mathbf{A} \quad -\mathbf{M}_{S^*}]^{-1}[\mathbf{H}_{S^*}][\mathbf{B}]\,\mathrm{d}\Gamma\{\Delta\} \tag{19}$$

Thus one can obtain the elastic stiffness matrix for the anchor from (19). In the boundary element formulation, however, the matrix $[\mathbf{C}][\mathbf{A} \quad -\mathbf{M}_{S^*}]^{-1}[\mathbf{H}_{S^*}]$ will not be symmetric due to the various numerical approximations involved. Therefore a least square technique has to be used to symmetrize the resulting stiffness matrices. The stiffness matrix of the rigid anchor can be written as

$$[\mathbf{K}] = \int_{S^*} [\mathbf{B}]^{\mathrm{T}}[\mathbf{D}^*][\mathbf{B}]\,\mathrm{d}\Gamma \tag{20}$$

where

$$[\mathbf{D}^*] = \tfrac{1}{2}[[\{\mathbf{C}\}[\mathbf{A} \quad -\mathbf{M}_{S^*}]^{-1}\{\mathbf{H}_{S^*}\}]^{\mathrm{T}} + [\mathbf{C}][\mathbf{A} \quad -\mathbf{M}_{S^*}]^{-1}[\mathbf{H}_{S^*}]] \tag{21}$$

Therefore a complete 6×6 stiffness matrix can be obtained for an anchor region with an arbitrary shape. For the case of a flat elliptical anchor whose principal axes coincide with the cartesian axes x and y, [K] can be reduced to a diagonal form with four displacement modes; namely,

(i) $\{v_1, \omega_2\}^{\mathrm{T}}$
(ii) $\{v_2, \omega_1\}^{\mathrm{T}}$
(iii) $\{v_3\}$
(iv) $\{\omega_3\}$

Thus (19) can be written in the form

$$\{\mathbf{F}\} = -\begin{bmatrix} c_{11} & c_{12} & 0 & 0 & 0 & 0 \\ c_{21} & c_{22} & 0 & 0 & 0 & 0 \\ 0 & 0 & c_{33} & c_{34} & 0 & 0 \\ 0 & 0 & c_{43} & c_{44} & 0 & 0 \\ 0 & 0 & 0 & 0 & c_{55} & 0 \\ 0 & 0 & 0 & 0 & 0 & c_{66} \end{bmatrix} \begin{bmatrix} v_1 \\ \omega_2 \\ v_2 \\ \omega_1 \\ v_3 \\ \omega_3 \end{bmatrix} \tag{22}$$

This formally completes the boundary element analysis of the problem of a rigid elliptical disc shaped anchor embedded at an elastic bi-material geological interface. The boundary element discretization of the bi-material region containing the rigid elliptical anchor is shown in Figure 3. The locations of the outer boundaries $S^{(1)}$ and $S^{(2)}$ are made sufficiently large to simulate approximately the response of a halfspace region. This is achieved by calibrating the boundary element results with known exact solutions for certain anchor problems related to an infinite space region. At the interface region near the boundary of the anchor, the boundary element mesh is refined to take into account high stress gradients induced by the rigid character of the anchor. No attempt is made to incorporate any stress singularities applicable to bi-material regions, at the boundary of the rigid anchor. These investigations are relegated to further studies. In the present paper, constant triangular elements have been used in the boundary element formulation. The singular integrations over the local elements can be obtained very accurately by using an analytical mean. Furthermore, smaller elements have been used near the edge of the rigid anchor region in which high stress gradients are expected (Figure 3b). Also, it may be noted that in terms of the approximate evaluation of the stiffness of the rigid anchor, the contributions from the singular points are expected to be relatively small.

APPROXIMATE BOUNDS FOR THE ELASTIC STIFFNESSES OF THE EMBEDDING ELLIPTICAL ANCHOR

In this section we shall outline analytical techniques which can be used to provide either sets of bounds or approximate estimates for the elastic stiffnesses of the rigid elliptical disc anchor embedded at a bi-material geological interface. These results will be used to estimate the relative accuracy of the boundary elements modelling of the problem. The stiffness bounds are obtained for the cases in which the rigid elliptical anchor is subjected to a rigid body displacement Δ_z in the z-direction and a rigid body rotation Ω_y about the y-axis. We shall also record here an approximate solution for the stiffness of the anchor which is subjected to a rotation free rigid body translation Δ_x in the x-direction. In the ensuing, attention is focused on the analytical derivation of the bounds that are applicable for the rigid displacement of the anchor in the z-direction. The bounds and/or results for other modes of deformation will only be presented in their final forms. Furthermore, it may be noted that the results derived from the ensuing analytical studies do not take into account the influences of the boundaries $S^{(1)}$ and $S^{(2)}$ which are present in the boundary element analysis. As the locations of $S^{(1)}$ and $S^{(2)}$ become remote from the anchor region, their influences are expected to be negligible.

Axial displacement of the elliptical anchor

Upper bound. The upper bound solution corresponds to the situation in which the bi-material geological interface exhibits inextensibility conditions (Figure 5a). Since the anchor is assumed

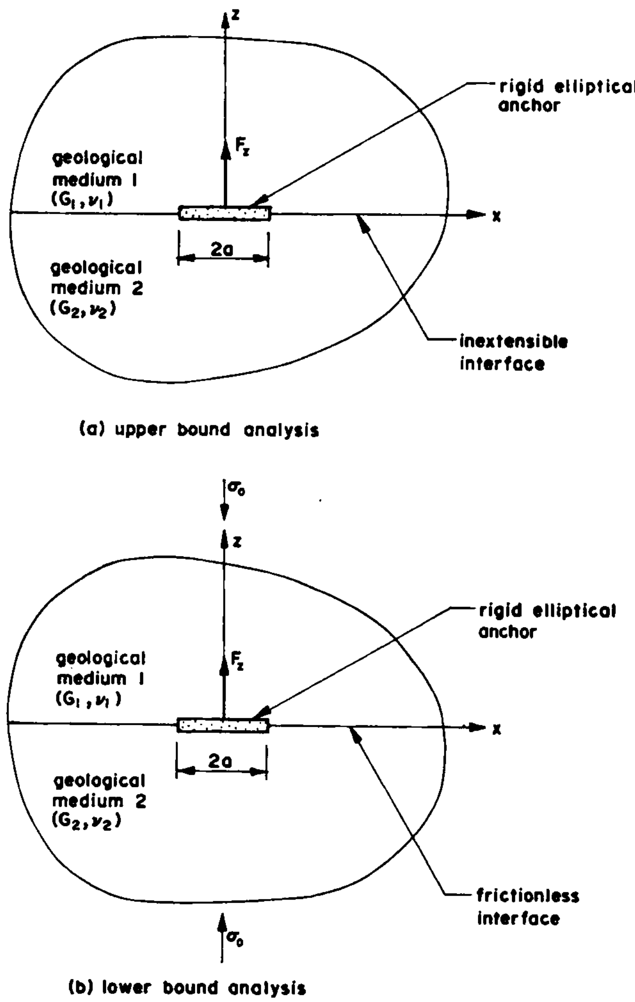

Figure 5. Upper and lower bound models for the analysis of the embedded anchor

to be rigid and the interface is considered to be inextensible, the conditions pertaining to displacements and tractions on S $(= S^* \cup \tilde{S})$ are as follows: we have

$$u_x^{(1)}(x,y,0) = u_x^{(2)}(x,y,0) = 0; \qquad (x,y)\in S \tag{23}$$

$$u_y^{(1)}(x,y,0) = u_y^{(2)}(x,y,0) = 0; \qquad (x,y)\in S \tag{24}$$

$$u_z^{(1)}(x,y,0) = u_z^{(2)}(x,y,0); \qquad (x,y)\in S \tag{25}$$

and

$$u_z^{(1)}(x,y,0) = u_z^{(2)}(x,y,0) = \Delta_z; \qquad (x,y)\in S^* \tag{26}$$

$$\sigma_{zz}^{(1)}(x,y,0) = \sigma_{zz}^{(2)}(x,y,0); \qquad (x,y)\in \tilde{S} \tag{27}$$

For the category of deformations which satisfy the constraints (23) and (24), the displacement and stress fields can be represented in terms of a single function $\Psi^{(\alpha)}(x,y,z)$ $(\alpha = 1,2)$ such that

$$u_z^{(\alpha)} = -(3-4\nu_\alpha)\Psi^{(\alpha)} + z\frac{\partial \Psi^{(\alpha)}}{\partial z} \tag{28}$$

$$\sigma_{zz}^{(\alpha)} = 2G_\alpha\left[-2(1-\nu_\alpha)\frac{\partial\Psi^{(\alpha)}}{\partial z} + z\frac{\partial^2\Psi^{(\alpha)}}{\partial z^2}\right] \tag{29}$$

Considering the boundary conditions (25)–(27) it can be shown that

$$\Psi^{(1)} = \left[\frac{3-4\nu_2}{3-4\nu_1}\right]\Psi^{(2)} = \Psi^* \tag{30}$$

and that the mixed boundary conditions on S yield the following:

$$\frac{\partial\Psi^*}{\partial z} = 0; \qquad (x,y)\in\tilde{S} \tag{31}$$

$$(3-4\nu_1)\Psi^* = -\Delta_z; \qquad (x,y)\in S^* \tag{32}$$

The details of the solution of (31) and (32) will not be pursued here; it can be shown that Ψ^* takes the general form

$$\Psi^*(x,y,z) = C\int_\xi^\infty \frac{\mathrm{d}s}{[s(a^2+s)(b^2+s)]^{1/2}} \tag{33}$$

where C is an arbitrary constant, (ξ,η,ζ) are the ellipsoidal co-ordinates of the point (x,y,z) and are the roots of

$$\frac{x^2}{(a^2+\theta)} + \frac{y^2}{(b^2+\theta)} + \frac{z^2}{\theta} - 1 = 0 \tag{34}$$

The constant C can be determined by making use of the boundary conditions (32). The stress and displacements in the elastic halfspace regions can be determined from (28), (29) and (33). The upper bound estimate for the stiffness of the elliptical rigid disc inclusion can be obtained by evaluating the resultant force acting on the faces of the inclusion, i.e.

$$F_z = \iint_{S^*} [\sigma_{zz}^{(1)}(x,y,0) - \sigma_{zz}^{(2)}(x,y,0)]\,\mathrm{d}x\,\mathrm{d}y \tag{35}$$

Lower bound. The lower bound is obtained by assuming that the interface region S exhibits frictionless conditions. The inclusion is therefore embedded at a frictionless bi-material interface. It is also assumed that the application of the load P does not cause separation at the interface. To achieve this, the bi-material regions are subjected to a sufficiently large uniform pre-compression σ_0 (Figure 5b). Since the analysis is restricted to linearly elastic behaviour, the stiffness of the inclusion is unaffected by σ_0 provided no separation occurs in S. The traction boundary conditions at the interface are

$$\sigma_{xz}^{(1)}(x,y,0) = \sigma_{xz}^{(2)}(x,y,0) = 0; \qquad (x,y)\in S \tag{36}$$

$$\sigma_{yz}^{(1)}(x,y,0) = \sigma_{yz}^{(2)}(x,y,0) = 0; \qquad (x,y)\in S \tag{37}$$

$$\sigma_{zz}^{(1)}(x,y,0) = \sigma_{zz}^{(2)}(x,y,0); \qquad (x,y)\in\tilde{S} \tag{38}$$

The displacement boundary conditions are

$$u_z^{(1)}(x,y,0) = u_z^{(2)}(x,y,0); \qquad (x,y)\in\tilde{S} \tag{39}$$

$$u_z^{(2)}(x,y,0) = u_z^{(2)}(x,y,0) = \Delta_z; \qquad (x,y)\in S^* \tag{40}$$

The reduced mixed boundary value problem posed by (38) and (40) can be analysed by employing the techniques outlined previously in connection with the upper bound problem.

Bounds for the axial elastic stiffness. Considering the techniques presented in the preceding sections, it can be shown that the axial load displacement response of a rigid elliptical disc inclusion embedded in bonded contact at a bi-material elastic interface can be presented in the form of the following set of bounds:

$$\frac{2\{(1-\nu_1)(3-4\nu_2)+R(1-\nu_2)(3-4\nu_1)\}}{(3-4\nu_1)(3-4\nu_2)(1+R)} \geqslant \bar{F}_z \geqslant \frac{\{(1-\nu_2)+R(1-\nu_1)\}}{2(1-\nu_1)(1-\nu_2)(1+R)} \tag{41}$$

where

$$\bar{F}_z = \frac{F_z}{4\pi\Delta_z a(G_1+G_2)/K(e_0)}; \qquad R = \frac{G_2}{G_1} \tag{42}$$

and $K(e_0)$ is the complete elliptic integral[12] of the first kind and $e_0^2 = (a^2 - b^2)/a^2$. It may be noted that as $\nu_\alpha \to 1/2$, the bounds (41) converge to the single result

$$F_z = \frac{4\pi\Delta_z a(G_1+G_2)}{K(e_0)} \tag{43}$$

Also, when $\nu_\alpha = \nu$ and $G_\alpha = G$, the asymmetry of the deformation ensures that $u_x = u_y = 0$ on $(x, y) \in S$; consequently the upper bound yields the exact solution for the elastic stiffness of a rigid elliptical disc shaped anchor region embedded in an isotropic elastic geological medium; i.e.

$$F_z = \frac{16\pi G(1-\nu)\Delta_z a}{(3-4\nu)K(e_0)} \tag{44}$$

Asymmetric rotation of the elliptical anchor

Upper bound. In the evaluation of the upper bound solution, it is assumed that the bi-material geological interface exhibits inextensibility conditions. Since the anchor is considered to be rigid on the interface extensible, the conditions pertaining to displacement and tractions on S are as follows:

$$u_x^{(1)}(x,y,0) = u_x^{(2)}(x,y,0); \qquad (x,y)\in S \tag{45}$$

$$u_y^{(1)}(x,y,0) = u_y^{(2)}(x,y,0); \qquad (x,y)\in S \tag{46}$$

$$u_z^{(1)}(x,y,0) = u_z^{(2)}(x,y,0); \qquad (x,y)\in S \tag{47}$$

and

$$u_z^{(1)}(x,y,0) = u_z^{(2)}(x,y,0) = \Omega_y x; \quad (x,y)\in S^* \tag{48}$$

$$\sigma_{zz}^{(1)}(x,y,0) = \sigma_{zz}^{(2)}(x,y,0); \qquad (x,y)\in \tilde{S} \tag{49}$$

The analysis of the mixed boundary value problem characterized by (48) and (49) follows the procedures outlined earlier. Considering the kinematic constraints (45)–(47), the mixed boundary conditions can be reduced to the following set of equations for an unknown function Ψ^*:

$$\frac{\partial \Psi^*}{\partial z} = 0; \qquad (x,y)\in \tilde{S} \tag{50}$$

$$(3-4\nu_1)\Psi^* = -\Omega_y x; \qquad (x,y)\in S^* \tag{51}$$

The analysis of the above mixed boundary value problem can be performed by formulating the problem in relation to an ellipsoidal co-ordinate system. The relevant solution for Ψ^* is given by

$$\Psi^* = Cx\int_\xi^\infty \frac{ds}{(a^2+s)[s(a^2+s)(b^2+s)]^{1/2}} = \frac{2Cx[u-E(u)]}{a^3 e_0^2} \tag{52}$$

where C is an arbitrary constant and $e_0^2 = (a^2 - b^2)/a^2$. The variable u is related to the ellipsoidal co-ordinate ξ by

$$\xi^2 = a^2(sn^{-2}u - 1) \tag{53}$$

$$E(u) = \int_0^u dn^2 t\, dt \tag{54}$$

The quantities $sn\,u$, $dn\,u$, etc., represent the Jacobian elliptic functions[13] which have real and imaginary roots $4K$ and $2iK$, respectively, corresponding to the moduli e_0 and $e_0^1 = b/a$. It may also be noted that $E(e_0)$ is the complete elliptic integral of the second kind.[12] Considering the boundary condition (48) and (52), it is possible to determine the constant C. Avoiding details of calculations, the normal stress in the anchor region in contact with the geological medium 1 is given by

$$\sigma_{zz}^{(1)}(x, y, 0) = \frac{4G_1(1-\nu_1)e_0^2 x\Omega_y}{(3-4\nu_1)b\left\{1 - \frac{x^2}{a^2} - \frac{y^2}{b^2}\right\}^{1/2}[K(e_0) - E(e_0)]} \tag{55}$$

The upper bound estimate for the rotational stiffness of the embedded elliptical anchor is obtained by evaluating the resultant of moments of $\sigma_{zz}^{(\alpha)}$ about the y axis; i.e.

$$M_y = \iint_{S^*} [\sigma_{zz}^{(1)}(x, y, 0) - \sigma_{zz}^{(2)}(x, y, 0)]\, x\, dx\, dy \tag{56}$$

With the knowledge that the rotation Ω_y occurs in the direction of application of M_y it can be shown that

$$M_y = \frac{8\pi a^3 G_1 e_0^2 \Omega_y}{3[K(e_0) - E(e_0)]}\left\{\frac{(1-\nu_1)(3-4\nu_2) + R(1-\nu_2)(3-4\nu_1)}{(3-4\nu_1)(3-4\nu_2)}\right\} \tag{57}$$

Lower bound. The lower bound for the rotational stiffness of the embedded elliptical anchor is obtained by invoking a frictionless bi-lateral contact at the geological interface. It is assumed that the application of the moment M_y does not cause separation at the smooth interface. Again, this constraint can be physically realized by subjecting the frictionless interface to a sufficiently large uniform precompression. Following the analytical procedures outlined in the preceding sections, it can be shown that the lower bound for the rotational stiffness of the embedded anchor region is given by

$$M_y = \frac{2\pi a^3 G_1 e_0^2 \Omega_y}{3[K(e_0) - E(e_0)]}\left\{\frac{(1-\nu_2) + R(1-\nu_1)}{(1-\nu_1)(1-\nu_2)}\right\} \tag{58}$$

Bounds for the rotational stiffness. From the results presented here, it is proposed that the bounds for the rotational stiffness of the elliptical anchor embedded at the geological interface can be presented in the form

$$2\left\{\frac{(1-\nu_1)(3-4\nu_2) + R(1-\nu_2)(3-4\nu_1)}{(3-4\nu_1)(3-4\nu_2)(1+R)}\right\} \geqslant \frac{3M_y\{K(e_0) - E(e_0)\}}{4\pi a^3 \Omega_y (G_1 + G_2)e_0^2} \geqslant \left\{\frac{(1-\nu_2) + R(1-\nu_1)}{2(1-\nu_1)(1-\nu_2)(1+R)}\right\} \tag{59}$$

It is of interest to note that the set of bounds (equation 59) that is developed for the rotational stiffness of the elliptical rigid anchor embedded at the bi-material interface is identical to the equivalent set developed for the axial stiffness of the elliptical anchor (equation 41).

Again, it can be shown that as $\nu_\alpha \to \frac{1}{2}$, the bounds converge to the single result

$$M_y = \frac{4\pi a^3 \Omega_y (G_1 + G_2) e_0^2}{3[K(e_0) - E(e_0)]} \tag{60}$$

Also, when $G_\alpha = G$ and $\nu_\alpha = \nu$, the asymmetry of the deformation imposes an inextensibility constraint on the plane $z = 0$; consequently, the upper bound gives the exact result

$$M_y = \frac{16\pi G a^3 \Omega_y (1-\nu) e_0^2}{3(3-4\nu)[K(e_0) - E(e_0)]} \tag{61}$$

It should be noted that during the application of the moment M_y, the rigid anchor embedded at the bi-material geological interface can, in general, experience a lateral translation Δ_x^* and an axial displacement Δ_z^* (these displacements are referred to the origin or centre of the embedded anchor). From symmetry considerations it can be shown that the axial displacement Δ_z^* is a second-order contribution which is not relevant to the linear elastic analysis of the embedded anchor problem. The lateral translation is, however, a non-trivial first-order contribution which should be estimated from a complete analysis of the problem. In the estimation of the analytical bounds, Δ_x^* is suppressed. This constraint, however, has no effect on the M_y vs. Ω_y relationships derived via the bounding techniques. The boundary element formulation of the elliptical anchor problem, however, correctly accounts for this coupling effect.

Lateral translation of the elliptical anchor

The analytical techniques described earlier could be further applied to develop an approximate relationship for the lateral load–displacement relationship of the elliptical anchor embedded at the bi-material geological interface. In order to develop the approximate analytical estimate for the lateral load–displacement relationship, we impose the following kinematic and traction constraints at the interface; i.e.

$$u_z^{(1)}(x,y,0) = u_z^{(2)}(x,y,0) = 0; \qquad (x,y) \in S \tag{62}$$

$$\sigma_{xz}^{(1)}(x,y,0) = \sigma_{xz}^{(2)}(x,y,0) = 0; \qquad (x,y) \in \tilde{S} \tag{63}$$

$$\sigma_{yz}^{(1)}(x,y,0) = \sigma_{yz}^{(2)}(x,y,0) = 0; \qquad (x,y) \in \tilde{S} \tag{64}$$

and

$$u_x^{(1)}(x,y,0) = u_x^{(2)}(x,y,0) = \Delta_x; \qquad (x,y) \in S^* \tag{65}$$

$$u_y^{(1)}(x,y,0) = u_y^{(2)}(x,y,0) = 0; \qquad (x,y) \in S^* \tag{66}$$

The mixed boundary value problem associated with (62)–(66) can be solved by using an ellipsoidal co-ordinate formulation described previously. Avoiding details of calculation, it can be shown that the approximate relationship between F_x and Δ_x can be evaluated in the form

$$F_x = \frac{8\pi a \Delta_x G_1 e_0^2}{[\{(3-4\nu_1)e_0^2 + 1\}K(e_0) - E(e_0)]}\{(1-\nu_1) + R(1-\nu_2)\chi\} \tag{67}$$

where

$$\chi = \left[\frac{\{(3-4\nu_1)e_0^2 + 1\}K(e_0) - E(e_0)}{\{(3-4\nu_2)e_0^2 + 1\}K(e_0) - E(e_0)}\right] \tag{68}$$

It may be noted that, in general, the application of the lateral force F_x induces not only a lateral translation Δ_x but also a rotation Ω_y^*, about the y-axis. This rotation is suppressed in the approximate solution (67), by virtue of the imposed constraint on u_z (given by (62)). Again, the analytical result for the rotation Ω_y^* can be obtained only via an exact analysis of the complete (unconstrained) mixed boundary value problem related to the bi-material region. The result (67) cannot be interpreted as a specific bound since both traction and kinematic constraints are imposed in S or $\tilde{S}$ of the interface region (see equations 62–64). The boundary element treatment of the problem yields the result for Ω_y^* and by virtue of Betti's reciprocal relationship

$$M_y \Omega_y^* = F_x \Delta_x^* \tag{69}$$

where Δ_x^* is the lateral translation due to the applied moment M_y.

NUMERICAL RESULTS

In this section we present a catalogue of numerical results which illustrate the manner in which the elastic properties of the bi-material geological region (G_α, ν_α; $\alpha = 1, 2$) influence the generalized

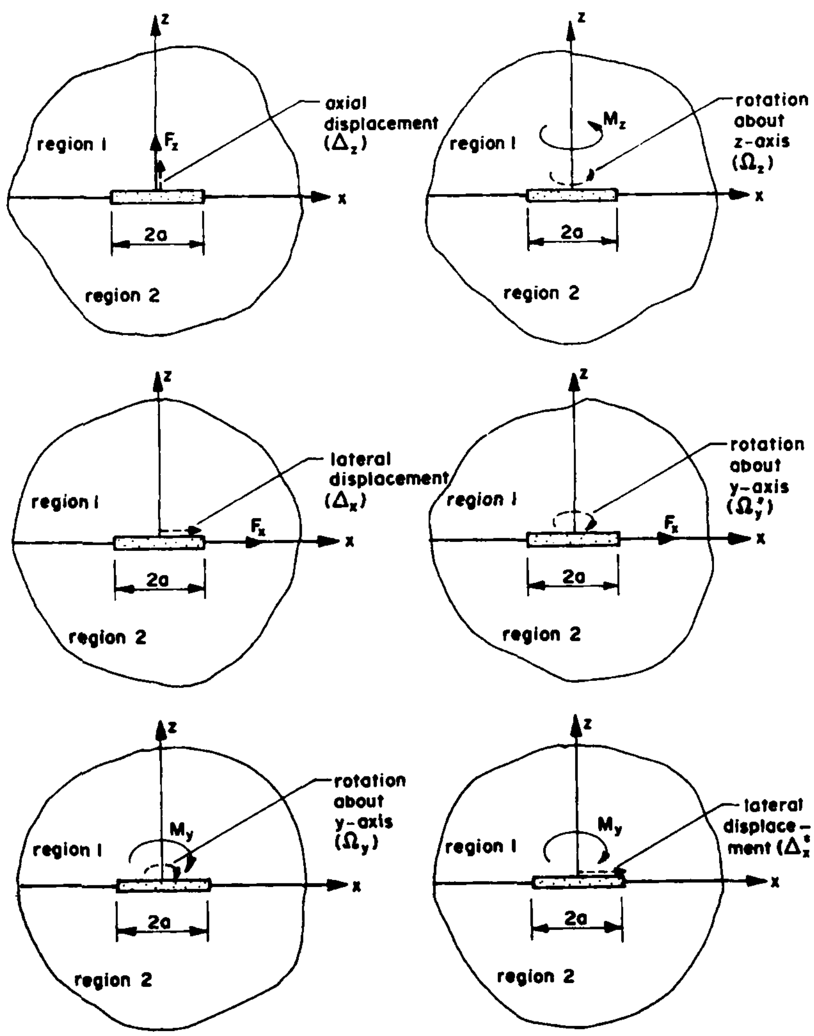

Figure 6. Generalized displacements of the elliptical anchor embedded at a bi-material geological interface

stiffness properties of the rigid elliptical anchor region. In the presentation of the numerical results, the effect of the anchor geometry is incorporated as a scale factor. The normalized forms for the load–displacement relationships are, in general, derived from the results obtained via the analytical techniques. Figure 6 illustrates the generalized displacements that are associated with the elliptical anchor embedded at the bi-material geological interface. For purposes of presentation of the numerical results it is convenient to introduce the following non-dimensional

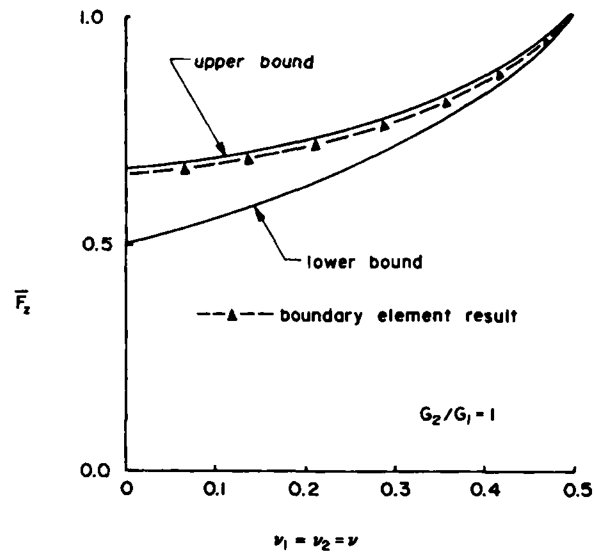

Figure 7. Axial stiffness of a rigid elliptical anchor embedded in a homogeneous geological medium

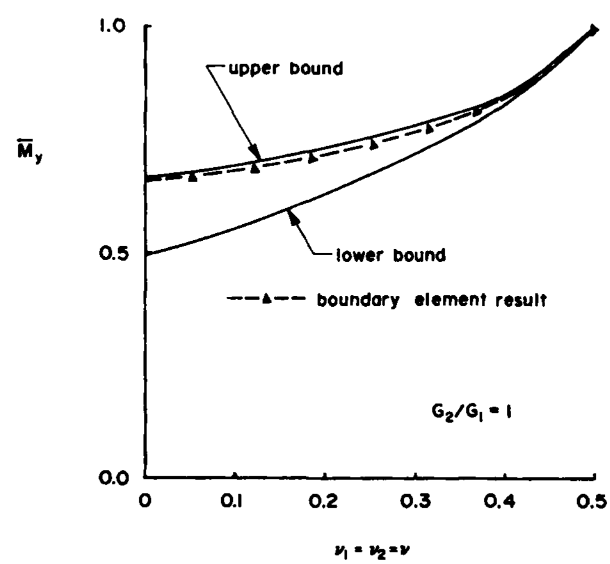

Figure 8. Rotational stiffness of a rigid elliptical anchor embedded in a homogeneous geological medium

variables:

$$\bar{F}_z = \frac{F_z}{4\pi a \Delta_z (G_1 + G_2)/K(e_0)} \tag{70a}$$

$$\bar{F}_x = \frac{F_x}{4\pi a \Delta_x (G_1 + G_2) e_0^2 / 3[K(e_0) - E(e_0)]} \tag{70b}$$

$$\bar{F}_x^* = \frac{F_x}{4\pi a^2 \Omega_y^* (G_1 + G_2) e_0^2 / 3[K(e_0) - E(e_0)]} \tag{70c}$$

$$\bar{M}_y = \frac{M_y}{4\pi a^3 \Omega_y (G_1 + G_2) e_0^2 / 3[K(e_0) - E(e_0)]} \tag{70d}$$

$$\bar{M}_z = \frac{M_z}{4\pi a^3 \Omega_z (G_1 + G_2)/K(e_0)} \tag{70e}$$

where $K(e_0)$ and $E(e_0)$ are complete elliptic integrals of the first and second kind. The reciprocal relationship can be used to estimate Δ_y^*.

The accuracy of the boundary element procedure and the boundary element discretization (Figure 3) was assessed by appeal to exact results derived for problems related to an elliptical rigid disc anchor embedded in an isotropic elastic solid. The analytical estimates for the axial, rotational and translational stiffnesses of a rigid elliptical anchor or a disc inclusion embedded in an isotropic elastic solid are given by Kassir and Sih[14] and Selvadurai.[15,16] Figures 7–9 illustrate the comparison of results derived for these stiffnesses via analytical and boundary element schemes. In all cases, the maximum discrepancy between the analytical and boundary element estimates is less than 2–3 per cent. This discrepancy, which is considered to

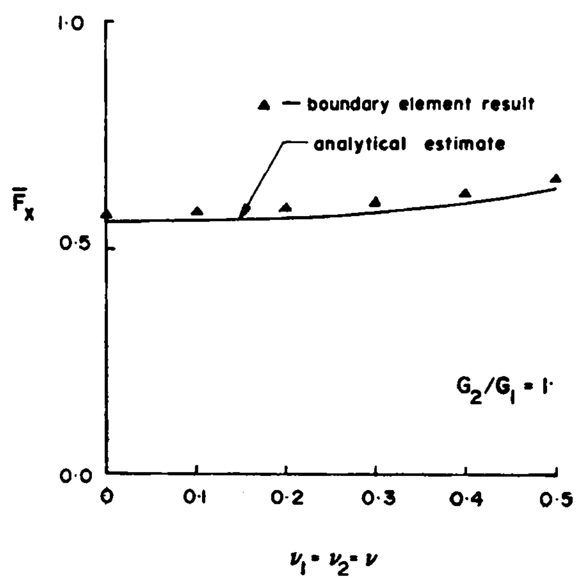

Figure 9. Lateral translational stiffness of a rigid elliptical anchor embedded in a homogeneous geological medium

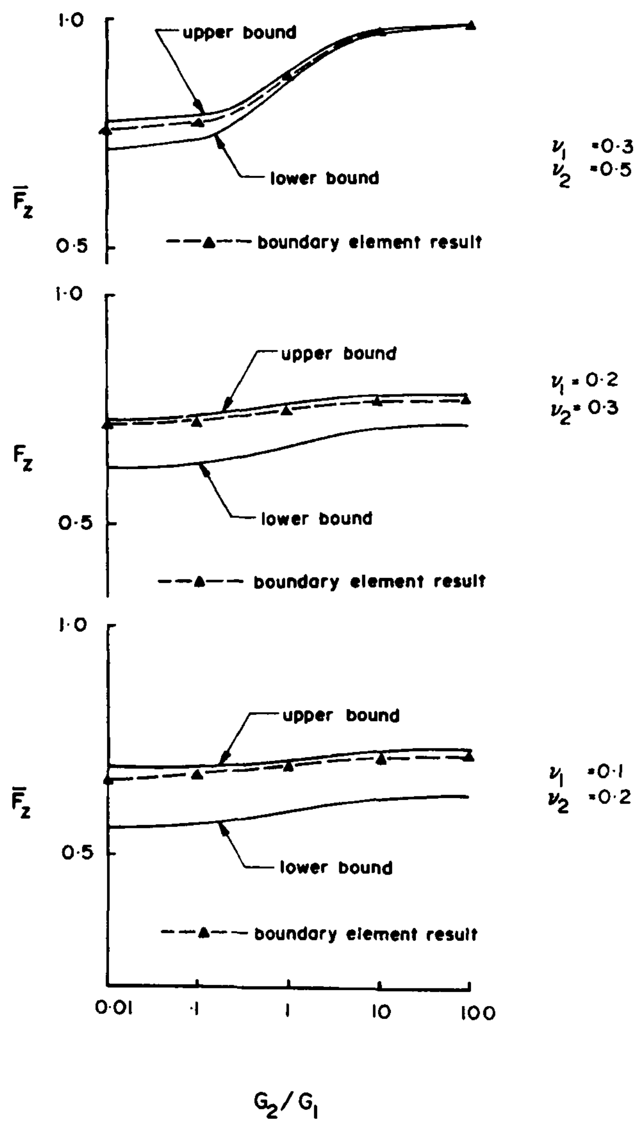

Figure 10. Axial stiffness of a rigid elliptical anchor embedded at a bi-material geological interface

be sufficient for engineering purposes, can be further reduced by using a refined boundary element discretization. In the ensuing numerical investigations, the boundary element discretization shown in Figure 3 is used.

Figure 10 illustrates the manner in which the normalized axial stiffnesses $\bar{F}_z$ of the rigid anchor are influenced by the elasticity mismatch between the two geological media. It is evident that the bounds developed via the analytical schemes provide suitable limits for the stiffnesses. As the Poisson's ratios of the geological media approach the limit of incompressibility ($\nu_\alpha = 1/2$), the bounds converge to a single result which agrees quite accurately with the boundary element estimate. Similar conclusions apply, in general, for the results for the non-dimensional rotational stiffness $\bar{M}_y$. Since the bounds for the axial stiffness are identical to the bounds for the rotational stiffness, the following relationship may be used to derive $M_y/\Omega_y a^2$ from F_z/Δ_z:

$$\frac{M_y}{\Omega_y a^2} = \frac{F_z K(e_0) e_0^2}{3\Delta_z \{K(e_0) - E(e_0)\}} \tag{71}$$

Relationship (71) applies only for the bounding estimates.

Figure 11 illustrates the boundary element results for the non-dimensional translational stiffness

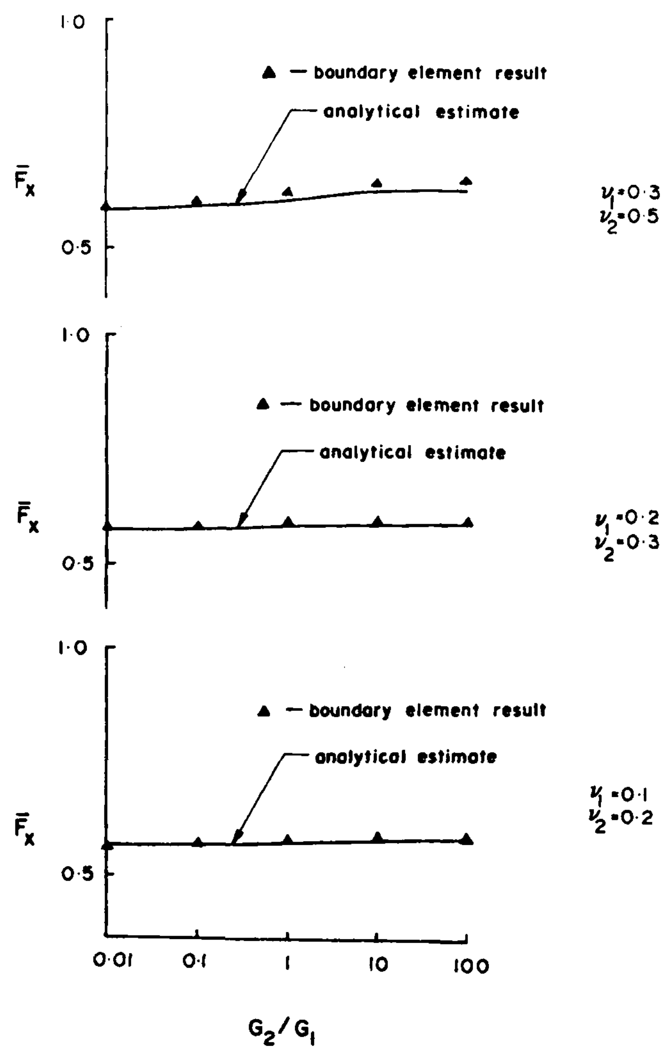

Figure 11. Translational stiffness of a rigid elliptical anchor embedded at a bi-material geological interface

of the elliptical rigid anchor embedded in a bi-material geological interface. The results for the single analytical estimate agree quite accurately with results of boundary element computations. The results for the torsional stiffness of the rigid elliptical anchor embedded at the geological interface are shown in Figure 12. Finally, Figure 13 illustrates the manner in which the elasticity mismatch between the geological media and the respective Poisson's ratios influence the coupling stiffness F_x^*; these results are obtained via the boundary element technique.

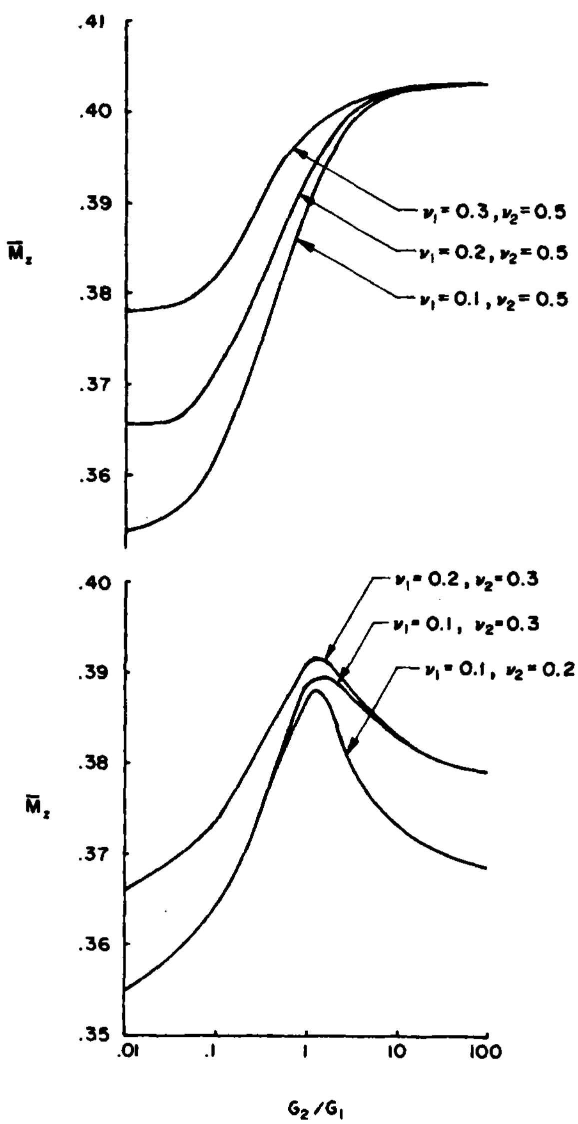

Figure 12. Torsional stiffness of a rigid elliptical anchor embedded at a bi-material geological interface

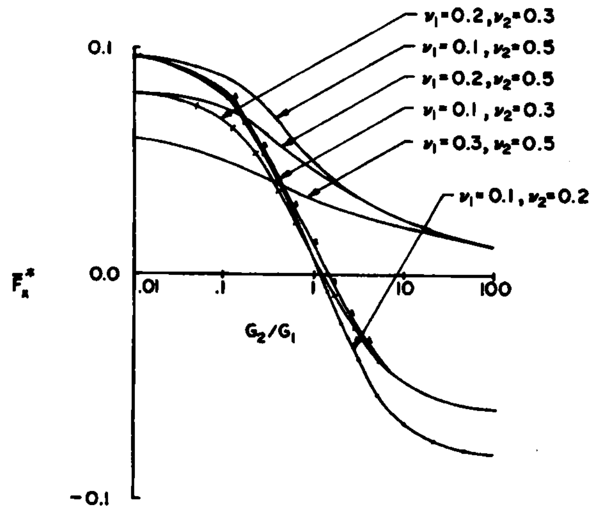

Figure 13. Coupling stiffness (rotation due to lateral force of a rigid elliptical anchor embedded at a bi-material geological interface

CONCLUSIONS

The class of problems which examine the interaction between rigid defect embedded at a bi-material elastic interface has useful application to the study of anchors embedded in soil and rock media. This paper presents two schemes for determining the generalized stiffness properties of such a rigid anchor, with an elliptical shape which is embedded in bonded contact at a bi-material geological interface. The analytical scheme focuses on the development of certain bounds for the elastostatic stiffnesses of the embedded anchor. The numerical scheme applies the boundary element technique to determine the generalized stiffness properties. The results presented here indicate that a relatively simplified boundary element scheme yields accurate estimates for the stiffness properties of the embedded anchor. The anchor geometry is restricted to an elliptical shape. Stiffness properties derived for such a shape can be used to obtain estimates for square, rectangular and elongated anchor regions embedded in geological media.

In the particular instance when $\nu_1 = \nu_2$, the set of bounds developed for the axial and rotational stiffness of the anchor (equations 41 and 59) become independent of the shear modular ratio R. It implies that if the values of Poisson's ratio in the two media are similar, then the stiffness of the anchor will not depend on R, however different the two shear moduli may be. In effect, the stiffness (both axial and rotational) will approach the stiffness of an anchor which is embedded in an 'effectively homogeneous' medium, whose shear modulus equals the average of the shear moduli of the two media. This conclusion appears to be of special interest, since it is unlikely that the values of Poisson's ratio in two adjacent rock layers will be greatly different. The shear moduli may be vastly different, but Poisson's ratios will probably differ very little. It then follows that nearly all practical problems involving a bi-material geological interface may be treated as anchors in a homogeneous medium with an effective shear modulus which averages the bi-material shear moduli.

ACKNOWLEDGEMENTS

The authors would like to thank the referees for their very valuable comments which led to significant improvements in the exposition of the conclusions. The work described in the paper was supported in part by a Natural Sciences and Engineering Research Council of Canada Grant A3866 on Soil–Structure Interaction.

REFERENCES

1. R. Butterfield and P. K. Banerjee, 'A rigid disc embedded in an elastic halfspace', *Geotech. Eng.*, **2**, 35–49 (1971).
2. S. C. Hunter and D. Gamblen, 'The theory of a rigid circular disc ground anchor buried in an elastic soil either with or without adhesion', *J. Mech. Phys. Solids*, **22**, 371–399 (1974).
3. A. P. S. Selvadurai, 'The load–deflexion characteristics of a deep rigid anchor in an elastic medium', *Geotech.*, **26**, 603–612 (1976).
4. A. P. S. Selvadurai, 'The eccentric loading of a rigid circular foundation embedded in an isotropic elastic medium', *Int. j. numer. anal. methods geomech.*, **4**, 121–129 (1980).
5. A. P. S. Selvadurai, 'The behaviour of anchor plates embedded in creep susceptible geological media', *Proc. Int. Symp. Weak Rock*, **2**, 769–775 (1981).
6. R. K. Rowe and E. H. Davis, 'Behaviour of anchor plates in clay', *Geotech.*, **32**, 9–23 (1982).
7. C. Truesdell, 'Invariant and complete stress functions for general continua', *Arch. Ration. Mech. Analysis*, **4**, 1–29 (1960).
8. M. E. Gurtin, 'The linear theory of elasticity', in *Mechanics of Solids II*, Encyclopaedia of Physics VIa/2 (ed. S. Flugge), Springer-Verlag, Berlin, 1972, 295 pp.
9. G. M. L. Gladwell, *Contact Problems in the Classical Theory of Elasticity*, Sijthoff and Noordhoff, Amsterdam, 1980.
10. C. Brebbia, *The Boundary Element Method for Engineers*, Pentech Press, London, 1978.
11. P. K. Banerjee and R. Butterfield, *Boundary Element Methods in Engineering Science*, McGraw-Hill, New York, 1981.
12. P. F. Byrd and M. D. Friedman, *Handbook of Elliptic Integrals*, Springer-Verlag, Berlin, 1971.
13. A. G. Greenhill, *The Applications of Elliptic Functions*, Dover Publications, New York, 1959.
14. M. K. Kassir and G. C. Sih, 'Some three-dimensional inclusion problems in elasticity', *Int. J. Solids Struct.*, **4**, 225–251 (1968).
15. A. P. S. Selvadurai, 'Axial displacement of a rigid elliptical disc inclusion embedded in a transversely isotropic elastic solid', *Mech. Res. Comm.*, **9**, 39–45 (1982).
16. A. P. S. Selvadurai, 'The rotation of a rigid elliptical disc inclusion embedded in a transversely isotropic elastic solid', *Mech. Res. Comm.*, **11** (1984) (in press).